


## Brief Communication

# CRISPR/Cas9-mediated generation of *fls2* mutant in *Nicotiana benthamiana* for investigating the flagellin recognition spectrum of diverse FLS2 receptors

Ling Wu, Hongju Xiao, Lijuan Zhao and Qiang Cheng\* 

Key Laboratory of Forest Genetics &amp; Biotechnology of Ministry of Education, Co-Innovation Center for Sustainable Forestry in Southern China, Nanjing Forestry University, Nanjing, China

Received 23 May 2022;

revised 11 July 2022;

accepted 22 July 2022.

\*Correspondence (Tel +86 025 85427891; fax +86 025 85427891; email chengqiang@njfu.edu.cn)

**Keywords:** Flagellin-sensing 2, flagellin epitope, *Nicotiana benthamiana*, CRISPR/Cas9, transient assay, reactive oxygen species burst.

Plant cell surface pattern-recognition receptors (PRRs) mount pattern-triggered immunity (PTI) by recognizing the typical molecular structures of pathogens, termed pathogen-associated molecular patterns (PAMPs), providing the first line of defence against various phytopathogens. Flagellin-sensing 2 (FLS2) of *Arabidopsis thaliana*, which perceives conserved epitopes (flg22) in the N-terminus of bacterial flagellin, was the first PRR to be identified (Gomez-Gomez and Boller, 2000). FLS2 homologues exist in most higher plants, but they differ in their recognition specificity. For example, tomato FLS2 can recognize flg15<sup>Eco</sup> derived from *Escherichia coli*, but Arabidopsis FLS2 cannot (Robatzek *et al.*, 2007). Flg22<sup>Agro</sup> of *Agrobacterium tumefaciens* avoids perception by most plants, whereas FLS2<sup>XL</sup> recently identified in wild grape can perceive this obstinate flagellin epitope. The interspecies transfer of FLS2<sup>XL</sup> can alter the specificity of flagellin perception in the recipient plant and enhance its resistance to *A. tumefaciens* (Fürst *et al.*, 2020).

The genome of allotetraploid tobacco *Nicotiana benthamiana* possesses two highly similar FLS2 genes (95.2% identity in coding sequences), *NbFLS2-1* (*Niben101Scf03455g01008*), and *NbFLS2-2* (*Niben101Scf01785g10011*; Bombarely *et al.*, 2012). We designed three single-guide RNAs (sgRNAs) to target both *NbFLS2-1* and *NbFLS2-2* (sgRNA1 and sgRNA3) or *NbFLS2-1* (sgRNA2). The sequences of *AtU6::sgRNAs* combined with 35S::Cas9 were inserted into the pCambia1300 vector (Appendix S1). Genetic transformations of *N. benthamiana* were performed. Three T1 lines, KO1&2 (transgenic sgRNA1 line, knockout of *NbFLS2-1* and *NbFLS2-2*), KO1 (sgRNA2, knockout of *NbFLS2-1*), and KO2 (sgRNA3, knockout of *NbFLS2-2*) were chosen because they were Cas9-free and carried homozygous frame-shift mutations. Although sgRNA2 also targeted *NbFLS2-2*, and sgRNA3 had only two mismatches with *NbFLS2-1*, these sgRNAs did not result in mutations of *NbFLS2-2* in KO1 and *NbFLS2-1* in KO2, respectively. The frame-shift mutations generated by CRISPR/Cas9 gene-editing lead to translation termination at the N-termini (102nd–254th amino acids) of the corresponding *NbFLS2s*,

suggesting their complete loss of function (Figure 1a–d). Furthermore, qRT-PCR results showed that the expression levels of mutated FLS2 genes were lower than that of wild type (Figure 1e).

To verify the *NbFLS2s*' loss of function, we performed three typical flagellin response experiments with leaf discs or seedlings of wild-type and KO lines. After flg22<sup>Psy</sup> (*Pseudomonas syringae*) treatments, wild type and KO1 generated reactive oxygen species (ROS) bursts (Figure 1f), accumulated activated MPK3/6 (Figure 1g), and exhibited significant growth inhibition (Figure 1h, i). In contrast, there were no obvious responses by KO1&2 and KO2. In addition, transient expression with 35S::g*NbFLS2* and 35S::g*NbFLS2::GFP* (g*NbFLS2*, the full-length genomic DNA sequences of *NbFLS2s*; GFP, coding sequence of green fluorescent protein) revealed that 35S::g*NbFLS2-2* and 35S::g*NbFLS2-2::GFP* can recover the ability to generate ROS bursts in KO1&2 after flg22<sup>Psy</sup> treatment, but 35S::g*NbFLS2-1* and 35S::g*NbFLS2-1::GFP* cannot (Figure 1j). Moreover, immunoblotting detected the accumulation of NbFLS2-2-GFP (~210 kDa) but did not detect NbFLS2-1-GFP (Figure 1k). RT-PCR and qRT-PCR results demonstrated the expression of two g*NbFLS2s* in transient assay (Figure S1a–c). Furthermore, no accumulation of target protein was observed in transient expression of the coding sequence of *NbFLS2-1* (Figure 1k). Therefore, the lack of function of *NbFLS2-1* may be due to translational level regulation.

Flagellin-induced ROS burst assays using *N. benthamiana* leaves that transiently express heterologous FLS2s represent a robust and convenient experimental method for identifying the function of FLS2s, but the presence of functional endogenous FLS2s, which can recognize a range of flagellin epitopes and/or may interact with downstream elements, limits the method's application. The *NbFLS2* double-mutant generated here can help overcome this limitation. We cloned the genomic DNA sequences of FLS2 homologues from multiple plants and generated binary vectors with the 35S::gFLS2::GFP construct. Their transient expression in KO1&2 revealed that 29 GFP-fused FLS2s (GenBank accession No. ON556647–ON556668, MH079052, MH079054, MH079055, MH079056 and MH079058) with molecular weights of approximately 200 to 210 kDa were successfully accumulated (Figure 1l). The leaf discs of KO1&2 expressing heterologous FLS2s were challenged with three flagellin epitopes (flg22<sup>Psy</sup>, flg15<sup>Eco</sup>, and flg22<sup>Agro</sup>) in ROS burst assays. Four FLS2 homologues failed to confer KO1&2 the ability to respond to flg22<sup>Psy</sup>, among which FLS2 from *Nelumbo nucifera*, *Kalanchoe laxiflora* and *Ginkgo biloba* lacked the 14–17th, 4–6th, and 26 & 28th LRR motifs, respectively, whereas *Morus alba* FLS2, lacking the 15th LRR motif and *Populus euphratica* FLS2, lacking the 26th LRR motif, still recognized flg22<sup>Psy</sup> (Figure 1m). In addition, there was

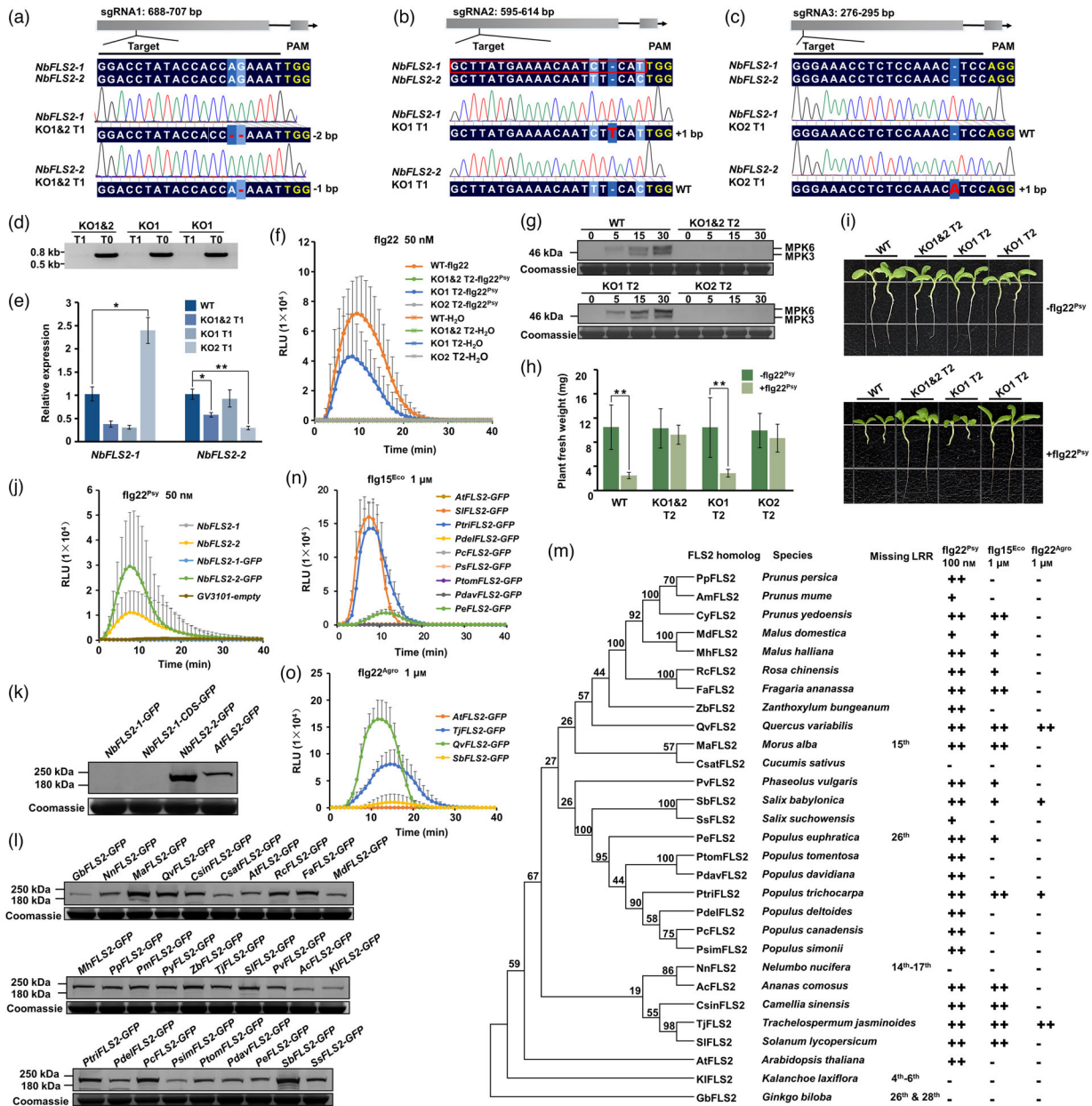


**Figure 1** Using CRISPR/Cas9 to knockout two *FLS2* genes in *N. benthamiana* and verify the functions of *FLS2*s from multiple plants. (a–c) Alignment of nucleotide sequences targeted by sgRNA1 (a), sgRNA2 (b), and sgRNA3 (c). Red letters and hyphens: insertions and deletions caused by Cas9/sgRNAs, respectively. DNA sequencing chromatograms of sgRNA target regions are provided for KO lines. The sequences of sgRNA1 and sgRNA3 are overlaid, and the sequence of sgRNA2 is indicated by the red rectangle. (d) Amplification of the Cas9 fragment with genomic DNAs of T0 and T1 lines. (e) The expression levels of *NbFLS2*s in wild type and KO lines as determined by qRT-PCR. Asterisks ( $P < 0.05$  and  $P < 0.01$ ) denote significant differences from the *NbFLS2* expression level of wild type (one-way ANOVA and Tukey’s test, with three independent experiments). (f) ROS burst assay with leaf discs after treatment with *flg22*<sup>Psy</sup> (50 nM) and H<sub>2</sub>O (mock). The error bars represent the means  $\pm$  SDs ( $n = 8$ ). (g) MAPK activation of leaf discs by *flg22*<sup>Psy</sup> (1  $\mu$ M) using a phospho-p44/42 MAPK antibody. (h, i) Fresh weight (h) and root length (i) of seedlings growing in liquid medium with and without *flg22*<sup>Psy</sup> (5  $\mu$ M) for 2 weeks. Asterisks ( $P < 0.05$  and  $P < 0.01$ ) denote significant differences from the fresh weight of *flg22*<sup>Psy</sup>-free seedlings of each line (one-way ANOVA and Tukey’s test,  $n > 10$ ). (j) ROS burst produced by KO1&2 leaves transiently expressing *NbFLS2*-GFPs and *NbFLS2*s after treatment with 50 nM *flg22*<sup>Psy</sup>. (k) Immunoblot of transiently expressing *NbFLS2*-GFPs in KO1&2 using an anti-GFP antibody. Transiently expressing *AtFLS2*-GFP served as control for molecular weight. (l) Immunoblot of 29 transiently expressing *FLS2*-GFPs in KO1&2 using an anti-GFP antibody. (m) ROS burst produced by KO1&2 leaves transiently expressing 7 *FLS2*-GFPs from *Populus* spp. after treatment with 1  $\mu$ M *flg22*<sup>Agro</sup>. Transiently expressing *SIFL2*-GFP and *AtFLS2*-GFP served as positive and negative controls of *flg22*<sup>Agro</sup> response, respectively. (n) ROS burst produced by KO1&2 leaves transiently expressing *QvFLS2*-GFP, *TJFLS2*-GFP, and *SbFLS2*-GFP after treatment with 1  $\mu$ M *flg22*<sup>Agro</sup>. Transiently expressing *AtFLS2*-GFP served as a negative control of the *flg22*<sup>Agro</sup> response. (o) Phylogeny of *FLS2* homologues. The phylogenetic tree was inferred using the maximum-likelihood method. Numbers at each node indicate the bootstrap percentage ( $n = 1000$ ). Missing LRRs, based on alignments with *AtFLS2*; RLU, relative light units; ++, RLU more than 50 000; +, RLU more than 10 000; –, RLU less than 10 000; ROS burst assays were performed using the luminol-based method with a GloMax™ 96 Microplate Luminometer. The full-length genomic sequences of *FLS2*s were used for all binary vector construction.

a difference in flg15<sup>Eco</sup> recognition among poplar FLS2s, i.e., FLS2 from *P. trichocarpa* and *P. euphratica* recognized flg15<sup>Eco</sup>, but FLS2s from five other poplar species did not (Figure 1n). Furthermore, FLS2 from *Quercus variabilis* and *Trachelospermum jasminoides* are highly sensitive to flg22<sup>Agro</sup> (Figure 1o).

Here, we used CRISPR/Cas9 technology to knock out two *FLS2* genes in *N. benthamiana* both separately and together, and we found that only NbFLS2-2 contributed to the recognition of flg22<sup>Psy</sup>. In addition, we combined transient expression and ROS burst assays to rapidly validate the FLS2 flagellin epitope recognition spectrum from 29 plant species in an *N. benthamiana* *FLS2* double-mutant. This convenient approach, combined with a large number of *FLS2* homologues currently revealed by plant genome sequencing, will facilitate screening of the FLS2s that can trigger broad-spectrum resistance or resistance targeting specific pathogens, and investigating co-evolutionary dynamics of plant FLS2 and bacterial flagellin in a given environment.

## Acknowledgement

This work was supported by the National Natural Science Foundation of China (Grant No. 31870658).

## Conflict of interest

The authors declare no conflict of interest.

## Author contributions

LW, HX, LZ, and QC performed research and analysed data, LW and QC wrote the paper. All the authors read and approved the manuscript.

## References

- Bombarely, A., Rosli, H.G., Vrebalov, J., Moffett, P., Mueller, L.A. and Martin, G.B. (2012) A draft genome sequence of *Nicotiana benthamiana* to enhance molecular plant-microbe biology research. *Mol. Plant Microbe Interact.* **25**, 1523–1530.
- Fürst, U., Zeng, Y., Albert, M., Witte, A.K., Fliegmann, J. and Felix, G. (2020) Perception of *Agrobacterium tumefaciens* flagellin by FLS2<sup>XL</sup> confers resistance to crown gall disease. *Nat. Plants*, **6**, 22–27.
- Gomez-Gomez, L. and Boller, T. (2000) FLS2: an LRR receptor-like kinase involved in the perception of the bacterial elicitor flagellin in *Arabidopsis*. *Mol. Cell*, **5**, 1003–1011.
- Robatzek, S., Bittel, P., Chinchilla, D., Köchner, P., Felix, G., Shiu, S.H. and Boller, T. (2007) Molecular identification and characterization of the tomato flagellin receptor LeFLS2, an orthologue of *Arabidopsis* FLS2 exhibiting characteristically different perception specificities. *Plant Mol. Biol.* **64**, 539–547.

## Supporting information

Additional supporting information may be found online in the Supporting Information section at the end of the article.

**Figure S1** Detecting the expression of *NbFLS2s* in transient assay.

**Appendix S1** Supplementary materials and methods.